PHYSICAL REVIEW B **80**, 081103(R) (2009)

Evidence for oxygen holes due to *d*-*p* rehybridization in thermoelectric $Sr_{1-x}Rh_2O_4$

Y. Ishida, T. Baba, R. Eguchi, M. Matsunami, M. Taguchi, and A. Chainani
RIKEN SPring-8 Center, Sayo, Sayo, Hyogo 679-5148, Japan

Y. Senba and H. Ohashi
JASRI/SPring-8, Sayo, Sayo, Hyogo 679-5198, Japan

Y. Okamoto
ISSP, University of Tokyo, Kashiwa-no-ha, Kashiwa, Chiba 277-8561, Japan

H. Takagi
RIKEN, The Institute for Physical and Chemical Research, Wako, Saitama 351-0198, Japan

S. Shin
RIKEN SPring-8 Center, Sayo, Sayo, Hyogo 679-5148, Japan
and ISSP, University of Tokyo, Kashiwa-no-ha, Kashiwa, Chiba 277-8561, Japan

(Received 29 April 2009; revised manuscript received 28 July 2009; published 12 August 2009)

Soft-x-ray photoemission and absorption spectroscopies are employed to investigate the electronic structures of $Sr_{1-x}Rh_2O_4$. Similar to the layered cobaltates such as $Na_{1-x}CoO_2$, a valence-band satellite feature (VBS) occurs at higher binding energy to the O 2*p* band. We find that the VBS resonates at the O 1*s* edge. Additionally, core absorption shows clear *x* dependence in the O 1*s* edge rather than in the Rh 3*p* edge. These results indicate that the holes in the initial state mainly have O 2*p* character presumably due to *d*-*p* rehybridizations affected by Sr^{2+} vacancy potentials. The resultant inhomogeneous charge texture may have impact on the thermoelectric transport properties at low *x*.

DOI: 10.1103/PhysRevB.80.081103   PACS number(s): 72.20.Pa, 71.27.+a, 79.60.−i

The search for efficient thermoelectric (TE) materials is extensively pursued with the aim at practical applications such as TE batteries and Peltier refrigerators.[1] Since metallic materials had been considered to exhibit poor TE performance,[1] it was a surprise that a low-resistive layered cobaltate $Na_{1-x}CoO_2$ ($x<0.5$) exhibited large TE power (Q) at high temperatures.[2,3] The cobaltates have gained further interest as exhibiting rich phase diagram[4] including superconductivity[5] and three-dimensional magnetism.[6,7] The largeness of Q has been discussed from a band-theoretical viewpoint[8–11] or from a correlated viewpoint,[12–15] or from a viewpoint that there is a coherent-to-incoherent crossover in the low-energy excitations with increasing T.[16,17] Furthermore, interesting Na orderings[18,19] that affect the electronic properties[20–22] have been reported, but their impact on the TE properties is not clear at present.

From a band-theoretical viewpoint, the valence band of $NaCoO_2$ consists of a filled t_{2g} band positioned just below the chemical potential (μ) and an O 2*p* band at higher binding energy (E_B) as schematically shown in the upper panel of Fig. 1(a). With Na^+ deintercalation, μ is shifted into the t_{2g} band, and holes of mainly t_{2g} character are introduced into the triangular lattice of Co^{3+} ions. Valence-band spectra of $Na_{0.7}CoO_2$ recorded by photoemission spectroscopy (PES) indeed show the t_{2g} and the O 2*p* bands, but in addition, there is a valence-band satellite feature (VBS) at $E_B \sim 11$ eV (Ref. 23) as schematically shown in the lower panel of Fig. 1(a). Similar VBSs occur in other layered cobaltates such as $LiCoO_2$ (Ref. 24) and $Ca_3Co_4O_9$ (Ref. 9) [VBSs in TE Bi-Sr-Co-O system are obscured by Bi 6*s* states at $E_B \sim 11$ eV (Ref. 25)]. Thus, the VBS is a ubiquitous feature in the TE cobaltates, which is missing in the band-theoretical density of states (DOS).

Herein, we investigate element-specific electronic structures of $Sr_{1-x}Rh_2O_4$ (Ref. 26) using soft-x-ray absorption (XAS) and resonant PES. $Sr_{1-x}Rh_2O_4$ is structurally and electronically analogous to $Na_{1-x}CoO_2$: hole carriers are introduced into the layered triangular lattice of low-spin Rh ions (nominally t_{2g}^6) through Sr^{2+} deintercalation [inset of Fig. 1(b)] to show insulator-to-metal transition at $x \sim 0.2$ [Fig. 1(b)], and the $x=0.22$ sample shows $Q \sim 70$ μV/K at 300 K [Fig. 1(c)].[26] Similarly to the cobaltates,[9,23,24] we find a VBS in $Sr_{1-x}Rh_2O_4$. Moreover, the VBS resonates at the O 1*s* edge followed by O 1*s*2*p*2*p* Auger emissions, providing strong constraints on its origin. We also find clear *x* dependence in the O 1*s* XAS rather than in the Rh 3*p* XAS. The results indicate that holes in $Sr_{1-x}Rh_2O_4$ have

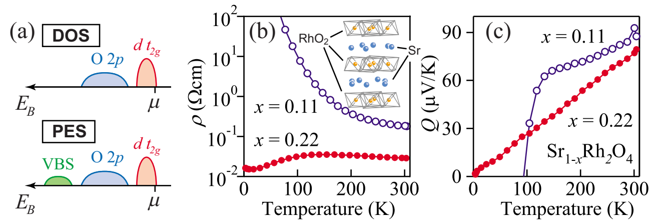

FIG. 1. (Color online) $Sr_{1-x}Rh_2O_4$, an analog of $Na_{1-x}CoO_2$. (a) Electronic structure. The band-theoretical DOSs of the cobaltates and the rhodates exhibit t_{2g} and O 2*p* bands, but the valence-band PES spectra additionally exhibit VBSs. (b) Resistivity and (c) TE power of $Sr_{1-x}Rh_2O_4$ as functions of temperature. The crystal structure of $SrRh_2O_4$ is shown in the inset of (b).

    ©2009 The American Physical Society

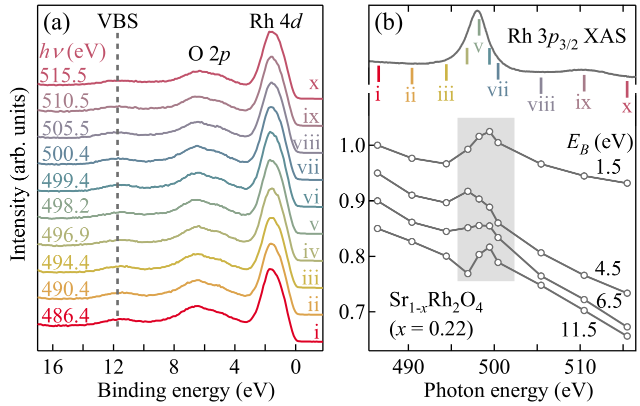

FIG. 2. (Color online) Rh $3p$-$4d$ resonant PES of $Sr_{1-x}Rh_2O_4$ (x=0.22). (a) Valence-band spectra recorded across the Rh $3p_{3/2}$ edge. (b) CIS spectra and Rh $3p_{3/2}$ XAS. CIS spectra are normalized to the intensity at 486.4 eV and have arbitrary offsets. The labels (i–x) on the spectra in (b) correspond to the photon energies indicated by bars on the Rh $3p_{3/2}$ XAS in (c).

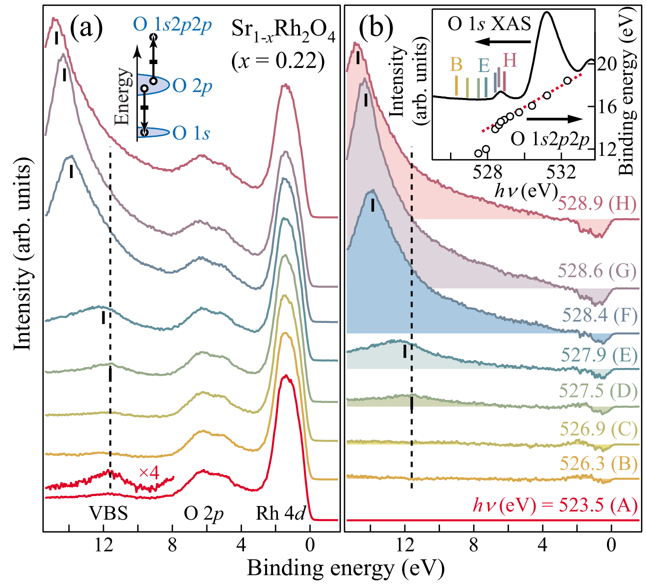

FIG. 3. (Color online) Valence-band spectra of $Sr_{1-x}Rh_2O_4$ (x =0.22) recorded across the O $1s$ edge. (a) Valence-band spectra recorded in the vicinity of the O $1s$ edge. Inset shows a schematic of the final state of an O $1s2p2p$ Auger-electron emission. (b) Difference spectra to the 523.0-eV spectrum. The labels (A–H) on the spectra correspond to the photon energies indicated on the O $1s$ XAS in the inset in (b). The dotted vertical lines indicate the 11.7 eV VBS, and the bars indicate the O $1s2p2p$ Auger peaks. The O $1s2p2p$ Auger peak positions are plotted in the inset in (b) in which the dotted line indicates the constant kinetic energy.

strong O $2p$ character presumably due to so-called d-p rehybridizations[27–30] that redistribute the holes from d states to p states beyond a rigid-band-shift picture.

Single-phase well-sintered $Sr_{1-x}Rh_2O_4$ (x=0.11 and 0.22) were prepared by a conventional solid-state reaction as described elsewhere.[26] The resistivity (ρ) and Q of the samples [Figs. 1(b) and 1(c), respectively] nicely reproduced those reported previously.[26] XAS and PES were performed at BL17SU of SPring-8 equipped with a VG Scienta SES2002 analyzer.[31] Sample surfaces were obtained by fracturing the samples inside the spectrometer under ultrahigh vacuum ($<5\times10^{-8}$ Pa). XAS spectra were recorded at 300K in the total electron yield method. PES spectra were recorded at 50 K at $\sim$250 meV energy resolution and E_B was referenced to μ of Au in contact with the sample and the analyzer. PES spectra were normalized to the incident photon flux.

Figure 2(a) shows valence-band spectra of $Sr_{1-x}Rh_2O_4$ (x=0.22) recorded across the Rh $3p_{3/2}$ edge. We find a VBS at $E_B\sim11.7$ eV, a feature missing in the local density approximation (LDA) DOS,[32] as well as the Rh $4d$ and the O $2p$ bands centered at $E_B\sim1.5$ and 6 eV, respectively. Figure 2(b) shows constant-initial-state (CIS) spectra at E_B =1.5, 4.5, 6.5, and 11.5 eV. One can see resonant enhancement of Rh $4d$ states at the Rh $3p_{3/2}$ edge [shaded area in Fig. 2(b)] in all features including the VBS (CIS at E_B =11.5 eV). This indicates that the Rh $4d$ weight is spread over a wide energy range and that the VBS has some Rh $4d$ character. The presence of the Co $3d$ character in the VBSs of the cobaltates was similarly confirmed through Co $3d$ resonant PES.[9,23,24]

Next, we performed resonant PES at the O $1s$ edge to obtain information about the O $2p$ states. Figures 3(a) and 3(b) show, respectively, the valence-band spectra recorded in the vicinity of the O $1s$ edge and the difference to the off-resonant spectra recorded at $h\nu$=523.0 eV. One can see that the VBS resonates at $h\nu$=527.5 eV and, subsequently, O $1s2p2p$ Auger peak emerges from the vicinity of the VBS. The results indicate that the final state of the 11.7 eV VBS is similar to that of the O $1s2p2p$ Auger emission, namely, the O $2p$-two-hole final state [see schematic in Fig. 3(a)]. This interpretation is the same as that of the 6 eV satellite of Ni identified to a Ni $3d$-two-hole final state.[33] In order to reach the O $2p$ two-hole final state by photoemission, the initial state should contain an electronic configuration that has a single hole in the O $2p$ state. We hereafter denote the initial oxygen-hole configuration as p_v^5. We note that the p_v^5 state is different from the ligand-hole states of the configuration-interaction CoO_6 cluster-model analyses[34,35] since the p_v^5 state is considered to be affected by the cation vacancy potentials[36] (discussed later). At $h\nu\geq528.7$ eV, the O $1s2p2p$ Auger peak position is shifted to higher E_B since the kinetic energy of an O $1s2p2p$ Auger electron is independent of $h\nu$ [inset in Fig. 3(c)]. The resonant peak position at $h\nu$=527.5 eV slightly deviates from the constant kinetic energy of the normal O $1s2p2p$ Auger, perhaps since the p_v^5 configuration is mixed to some d-hole configurations as inferred from the Rh $4d$ resonant PES (Fig. 2).

Evidence for oxygen holes in the initial state is also found in the XAS as shown in Fig. 4. With increasing x, the height of the prepeak feature in the O $1s$ XAS at $h\nu$=528.7 eV becomes large and that of the main peak at $h\nu$=531.2 eV becomes small (for each composition, the line shape at $h\nu$ <533 eV was reproducible for three fractures). On the other hand, the Rh $3p$ XAS is hardly changed with x. Since the O $1s$ prepeak intensity is almost in proportional to x, we assign it to Sr-vacancy induced states mainly having O $2p$ character so that the prepeak is assigned to $(1s^2)(2p_v^5)$ $\rightarrow(1s^1)(2p^6)$. The spectral-weight transfer seen in O $1s$ XAS

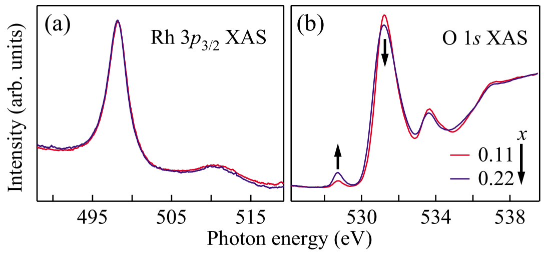

FIG. 4. (Color online) (a) Rh $3p_{3/2}$ and (b) O 1*s* XAS. The arrows in (b) indicate the change with increasing *x*.

is often taken as a signature of strong electron correlation.[34] In the XAS studies of $(Li/Na)_{1-x}CoO_2$,[37–39] main changes with *x* occurred in the O 1*s* XAS rather than in the Co 2*p* XAS. Thus, oxygen holes in the initial state are common features in the TE rhodates and cobaltates.

The oxygen holes in $Sr_{1-x}Rh_2O_4$ revealed by resonant PES and XAS at the O 1*s* edge indicate that the electronic-structure evolution with *x* goes beyond a rigid-band-shift picture. Otherwise, μ would shift with increasing *x* into the Rh 4*d* band resulting in holes that mainly have Rh 4*d* character. The spectral weight should therefore be redistributed with increasing *x*, most likely due to *d-p* rehybridization:[27–30] as evidenced from the charge densities calculated[40] for $Li_{1-x}CoO_2$ (Refs. 27 and 28) and $Na_{1-x}CoO_2$,[29] the holes introduced via Li/Na deintercalation are not homogeneously distributed in the Co layers but reside at oxygen sites neighboring the Li/Na vacancies; i.e., the cation vacancy potential binds the holes to form the p_v^5 state.[28] The charge density at a Co site was nearly unchanged with increasing *x* (Refs. 27–29) since the t_{2g} holes were dressed by e_g electrons transferred from the O 2*p* states through the *d-p* rehybridization. The essence of the charge rearrangement with doping can be captured in a simple model, namely, transition-metal impurities in semiconductors.[30,41] The rigidity of the Rh 3*p* XAS line shape with *x* [Fig. 4(a)] is thus considered as a fingerprint that the *d-p* rehybridization is self-regulating the local charge density about the Rh site to a nearly constant value.

A striking difference between the O 1*s* XAS of $Sr_{1-x}Rh_2O_4$ and those of $(Na/Li)_{1-x}CoO_2$ (Refs. 34 and 37–39) is that the *x*-dependent prepeak in the former is well separated from the main peak [Fig. 4(b)], whereas those in the latter are merging into the main peaks. This can be understood that the degree of localization of the p_v^5 state is affected by the strength of the cation vacancy potentials. Since the divalent Sr^{2+} vacancy potential is stronger than those of the monovalent Li^+/Na^+, the holes are more strongly bound around the vacancies in the former than in the latter.[28] Hence, the p_v^5 state appears to be more localized in $Sr_{1-x}Rh_2O_4$ so that the prepeak appears to be a sharp level. The localized character of the p_v^5 state is supported by an ^{17}O NMR study of $Na_{1-x}CoO_2$ ($x=0.28$), revealing that $\sim 30\%$ of the oxygen sites carry local magnetic moments.[42] We naturally identify these magnetic oxygens to have the p_v^5 configuration.

It should be noted that a VBS was also observed in stoichiometric $LiCoO_2$ having no Li vacancies.[24] Through a configuration-interaction cluster-model analysis, the VBS of $LiCoO_2$ was attributed to large *d-p* hybridization and orbital degeneracy of the *d* states.[24] Thus, the *d-p rehybridization* with doping effectively occurs when the parent compound has large *d-p* hybridization and orbital degeneracy. Large *d-p* hybridization generally occurs in t_{2g} electron system having unoccupied e_g orbitals (this includes d^0 insulators[43,44]). In fact, *d-p* rehybridization was reported to occur when carriers are doped into $SrTiO_3$, a nominally d^0 insulator.[45] It is also interesting that a layered Cu_xTiSe_2, which shows TE properties as good as the cobaltates,[46] is also considered to exhibit *d-p* rehybridization.[47] Here, the hybridization of the Se 4*p* states into the unoccupied Ti 3*d* states opens the channel of *d-p* rehybridization, and Cu^+ act as a source of "occupancy" potential. Thus, the TE cobaltates, rhodates, and the intercalated Ti dichalcogenides can be categorized to those exhibiting *d-p* rehybridization affected by the cation vacancy/occupancy potentials.

Since the holes in the initial state are not homogenously distributed in the Rh layers as expected in a rigid-band-shift picture but are further redistributed due to the *d-p* rehybridizations and the Sr-vacancy potentials, the charge density is considered to be nonperiodic compared to the crystallographic periodicity of $SrRh_2O_4$ [please see the nonperiodic charge densities calculated for $(Li/Na)_{1-x}CoO_2$ (Refs. 27–29)]. Thus, it would be necessary to realize that the transport is occurring on such an inhomogeneous charge texture with O 2*p* holes bound to cation vacancies. For example, as was pointed out in Ref. 32, the nonmetallic conduction at $x \lesssim 0.2$ of $Sr_{1-x}Rh_2O_4$ (Ref. 26) can be viewed as a variable-range hopping, i.e., the low-energy excitations relevant to the transport show weak localizations as they are subject to randomness.[48] The mobility-edge crossing occurring at $x \sim 0.2$ in $Sr_{1-x}Rh_2O_4$ is reasonably larger than that of $Na_{1-x}CoO_2$ occurring at $x < 0.1$ (Ref. 3) since the vacancy potential of Sr^{2+} is stronger than that of Na^+, although single-crystal data will be helpful for further investigations.[49] Another point to be noted is, when a nonmetallic transport is realized by randomness in a spin-orbitally degenerate system such as in $Fe_3O_{4-x}F_x$,[50] a hump feature occurs at $T \sim 100$ K in a *Q-T* curve.[49–51] This feature is very similar to the enhanced *Q* at ~ 100 K in metallic $Na_{1-x}CoO_2$ at low *x*,[3] which is considered to be on the verge of the metal-nonmetal transition. Further studies are necessary to clarify the relationship between the randomness and the transport properties in the rhodates and the cobaltates particularly at low *x*.

In summary, we have performed resonant PES and XAS on $Sr_{1-x}Rh_2O_4$ and find that the holes have strong O 2*p* character. The VBS, which commonly occurs in the TE cobaltates, is proven from resonant PES at the O 1*s* edge to be a fingerprint of the O 2*p* holes in the initial state. The results indicate a nonrigid-band evolution of the electronic structure with doping due to the *d-p* rehybridization affected by the cation vacancy potentials,[27–30] resulting in an inhomogeneous charge texture that may affect the transport properties at low *x*.

Y.I. acknowledges A. Mizutani, K. Sugiura, H. Ohta, and I. Matsuda for informative discussion and T. Mizokawa for critical reading of the manuscript.

[1] G. Mahan, B. Sales, and J. Sharp, Phys. Today **50** (3), 42 (1997).
[2] I. Terasaki, Y. Sasago, and K. Uchinokura, Phys. Rev. B **56**, R12685 (1997).
[3] Minhyea Lee, Liliana Viciu, Lu Li, Yayu Wang, M. L. Foo, S. Watauchi, R. A. Pascal, Jr., R. J. Cava, and N. P. Ong, Nature Mater. **5**, 537 (2006).
[4] M. L. Foo, Y. Wang, S. Watauchi, H. W. Zandbergen, T. He, R. J. Cava, and N. P. Ong, Phys. Rev. Lett. **92**, 247001 (2004).
[5] Kazunori Takada, Hiroya Sakurai, Eiji Takayama-Muromachi, Fujio Izumi, Ruben A. Dilanian, and Takayoshi Sasaki, Nature (London) **422**, 53 (2003).
[6] J. Sugiyama, J. H. Brewer, E. J. Ansaldo, B. Hitti, M. Mikami, Y. Mori, and T. Sasaki, Phys. Rev. B **69**, 214423 (2004).
[7] S. P. Bayrakci, I. Mirebeau, P. Bourges, Y. Sidis, M. Enderle, J. Mesot, D. P. Chen, C. T. Lin, and B. Keimer, Phys. Rev. Lett. **94**, 157205 (2005).
[8] D. J. Singh, Phys. Rev. B **61**, 13397 (2000).
[9] T. Takeuchi *et al.*, Phys. Rev. B **69**, 125410 (2004).
[10] H. J. Xiang and D. J. Singh, Phys. Rev. B **76**, 195111 (2007).
[11] K. Kuroki and R. Arita, J. Phys. Soc. Jpn. **76**, 083707 (2007).
[12] W. Koshibae, K. Tsutsui, and S. Maekawa, Phys. Rev. B **62**, 6869 (2000).
[13] Y. Wang, N. S. Rogado, R. J. Cava, and N. P. Ong, Nature (London) **423**, 425 (2003).
[14] O. I. Motrunich and P. A. Lee, Phys. Rev. B **69**, 214516 (2004).
[15] J. O. Haerter, M. R. Peterson, and B. S. Shastry, Phys. Rev. Lett. **97**, 226402 (2006).
[16] P. Limelette, S. Hebert, V. Hardy, R. Fresard, C. Simon, and A. Maignan, Phys. Rev. Lett. **97**, 046601 (2006).
[17] Y. Ishida, H. Ohta, A. Fujimori, and H. Hosono, J. Phys. Soc. Jpn. **76**, 103709 (2007).
[18] M. Roger *et al.*, Nature (London) **445**, 631 (2007).
[19] F. C. Chou, M. W. Chu, G. J. Shu, F. T. Huang, W. W. Pai, H. S. Sheu, and P. A. Lee, Phys. Rev. Lett. **101**, 127404 (2008).
[20] C. A. Marianetti and G. Kotliar, Phys. Rev. Lett. **98**, 176405 (2007).
[21] M. Gao, S. Zhou, and Z. Wang, Phys. Rev. B **76**, 180402(R) (2007).
[22] M.-H. Julien *et al.*, Phys. Rev. Lett. **100**, 096405 (2008).
[23] M. Z. Hasan *et al.*, Phys. Rev. Lett. **92**, 246402 (2004).
[24] J. van Elp, J. L. Wieland, H. Eskes, P. Kuiper, G. A. Sawatzky, F. M. F. de Groot, and T. S. Turner, Phys. Rev. B **44**, 6090 (1991).
[25] T. Mizokawa, L. H. Tjeng, P. G. Steeneken, N. B. Brookes, I. Tsukada, T. Yamamoto, and K. Uchinokura, Phys. Rev. B **64**, 115104 (2001).
[26] Y. Okamoto, M. Nohara, F. Sakai, and H. Takagi, J. Phys. Soc. Jpn. **75**, 023704 (2006).
[27] C. Wolverton and A. Zunger, Phys. Rev. Lett. **81**, 606 (1998).
[28] C. A. Marianetti, G. Kotliar, and G. Ceder, Nature Mater. **3**, 627 (2004).
[29] C. A. Marianetti, G. Kotliar, and G. Ceder, Phys. Rev. Lett. **92**, 196405 (2004).
[30] H. Raebiger, S. Lany, and A. Zunger, Nature (London) **453**, 763 (2008).
[31] H. Ohashi, Y. Senba, H. Kishimoto, T. Miura, E. Ishiguro, T. Takeuchi, M. Oura, K. Shirasawa, T. Tanaka, M. Takeuchi, K. Takeshita, S. Goto, S. Takahashi, H. Aoyagi, M. Sano, Y. Furukawa, T. Ohata, T. Matsushita, Y. Ishizawa, S. Taniguchi, Y. Asano, Y. Harada, T. Tokushima, K. Horiba, H. Kitamura, T. Ishikawa, and S. Shin, AIP Conf. Proc. **879**, 523 (2007).
[32] G. B. Wilson-Short, D. J. Singh, M. Fornari, and M. Suewattana, Phys. Rev. B **75**, 035121 (2007).
[33] C. Guillot, Y. Ballu, J. Paigne, J. Lecante, K. P. Jain, P. Thiry, R. Pinchaux, Y. Petroff, and L. M. Falicov, Phys. Rev. Lett. **39**, 1632 (1977).
[34] W. B. Wu, D. J. Huang, J. Okamoto, A. Tanaka, H. J. Lin, F. C. Chou, A. Fujimori, and C. T. Chen, Phys. Rev. Lett. **94**, 146402 (2005).
[35] T. Kroll, A. A. Aligia, and G. A. Sawatzky, Phys. Rev. B **74**, 115124 (2006).
[36] Since the charge densities of $Li_{1-x}CoO_2$ (Refs. 27 and 28) and $Na_{1-x}CoO_2$ (Ref. 29) are strongly affected by the cation vacancies, it is not *a priori* to adopt the symmetry of a CoO_6 octahedra (Refs. 34 and 35) to understand the electronic structures of the cobaltates.
[37] L. A. Montoro, M. Abbate, and J. M. Rosolen, Electrochem. Solid-State Lett. **3**, 410 (2000).
[38] V. R. Galakhov *et al.*, Phys. Rev. B **74**, 045120 (2006).
[39] T. Kroll, M. Knupfer, J. Geck, C. Hess, T. Schwieger, G. Krabbes, C. Sekar, D. R. Batchelor, H. Berger, and B. Buchner, Phys. Rev. B **74**, 115123 (2006).
[40] Even though LDA DOS cannot reproduce VBS since LDA does not treat dynamical correlations in the electron removal state (Ref. 52), charge densities, which are initial-state properties and are considered to be less affected by dynamical correlations, are nicely explained by LDAs.
[41] F. D. M. Haldane and P. W. Anderson, Phys. Rev. B **13**, 2553 (1976).
[42] F. L. Ning and T. Imai, Phys. Rev. Lett. **94**, 227004 (2005).
[43] K. Okada and A. Kotani, J. Phys. Soc. Jpn. **63**, 3176 (1994).
[44] M. Umeda, Y. Tezuka, S. Shin, and A. Yagishita, Phys. Rev. B **53**, 1783 (1996).
[45] Y. Ishida, R. Eguchi, M. Matsunami, K. Horiba, M. Taguchi, A. Chainani, Y. Senba, H. Ohashi, H. Ohta, and S. Shin, Phys. Rev. Lett. **100**, 056401 (2008).
[46] G. Wu, H. X. Yang, L. Zhao, X. G. Luo, T. Wu, G. Y. Wang, and X. H. Chen, Phys. Rev. B **76**, 024513 (2007).
[47] C. Umrigar, D. E. Ellis, D. S. Wang, H. Krakauer, and M. Posternak, Phys. Rev. B **26**, 4935 (1982).
[48] N. F. Mott, *Metal-Insulator Transitions*, 2nd ed. (Taylor & Francis, New York, 1990).
[49] Kenji Sugiura, Hiromichi Ohta, Yukiaki Ishida, Rong Huang, Tomohiro Saito, Yuichi Ikuhara, Kenji Nomura, Hideo Hosono, and Kunihito Koumoto, Appl. Phys. Express **2**, 035503 (2009).
[50] H. Graener, M. Rosenberg, T. E. Whall, and M. R. B. Jones, Philos. Mag. B **40**, 389 (1979).
[51] I. P. Zvyagin, in *The Hopping Thermopower in Hopping Transport in Solids*, Modern Problems in Condensed Matter Sciences, edited by M. Pollak and B. Shklovskii (North-Holland, Amsterdam, 1991), Vol. 28.
[52] J. Kunes, V. I. Anisimov, S. L. Skornyakov, A. V. Lukoyanov, and D. Vollhardt, Phys. Rev. Lett. **99**, 156404 (2007).